Séminaire Lotharingien de Combinatoire **86B** (2022)
Article #8, 12 pp.

Proceedings of the 34th Conference on Formal Power Series and Algebraic Combinatorics (Bangalore)

Walks in Simplices, Cylindric Tableaux, and Asymmetric Exclusion Processes

Sergi Elizalde*

Department of Mathematics, Dartmouth College, Hanover, NH 03755, USA.

Abstract. We establish bijections between three classes of combinatorial objects that have been studied in different contexts: lattice walks in simplicial regions as introduced by Mortimer–Prellberg, standard cylindric tableaux as introduced by Gessel–Krattenthaler and Postnikov, and sequences of states in the totally asymmetric simple exclusion process. This perspective gives new insights into these objects, providing a vehicle to translate enumerative results from lattice walks to tableaux, and to interpret symmetries that are natural in one setting (*e.g.* conjugation of tableaux) as involutions in another. Specifically, it allows us to use a cylindric analogue of the Robinson–Schensted correspondence to give an alternative bijective proof of a recent result of Courtiel, Elvey Price and Marcovici relating forward and backward walks in simplices.

Keywords: constrained walk, cylindric tableau, cylindric RSK, TASEP

1 Introduction

1.1 Walks in simplices

For positive integers d and L, define the following simplicial section of the d-dimensional integer lattice:

$$\Delta_{d,L} = \{(x_1, x_2, \ldots, x_d) \in \mathbb{N}^d : x_1 + x_2 + \cdots + x_d = L\},$$

where $\mathbb{N}$ is the set of non-negative integers. For $1 \le i \le d$, let e_i be the unit vector whose ith coordinate equals 1 and whose other coordinates equal 0, and let $s_i = e_{i+1} - e_i$,[1] with the convention $e_{d+1} = e_1$. See the left of Figure 1 for an example. We consider walks in $\Delta_{d,L}$ with steps s_i for $1 \le i \le d$; equivalently, walks in the directed graph $\mathcal{D}_{d,L}$ whose vertices are the points in $\Delta_{d,L}$, and whose edges are ordered pairs $(\mathbf{x}, \mathbf{y})$ such that $\mathbf{y} - \mathbf{x} = s_i$ for some i. The graph $\mathcal{D}_{3,3}$ appears in Figure 2(b). Let $C = (L, 0, \ldots, 0) \in \Delta_{d,L}$ be a corner of the simplex.

*sergi.elizalde@dartmouth.edu.

[1] This indexing differs from the notation in [2] in that it is shifted by one, but it is more convenient for our correspondences with other combinatorial objects.

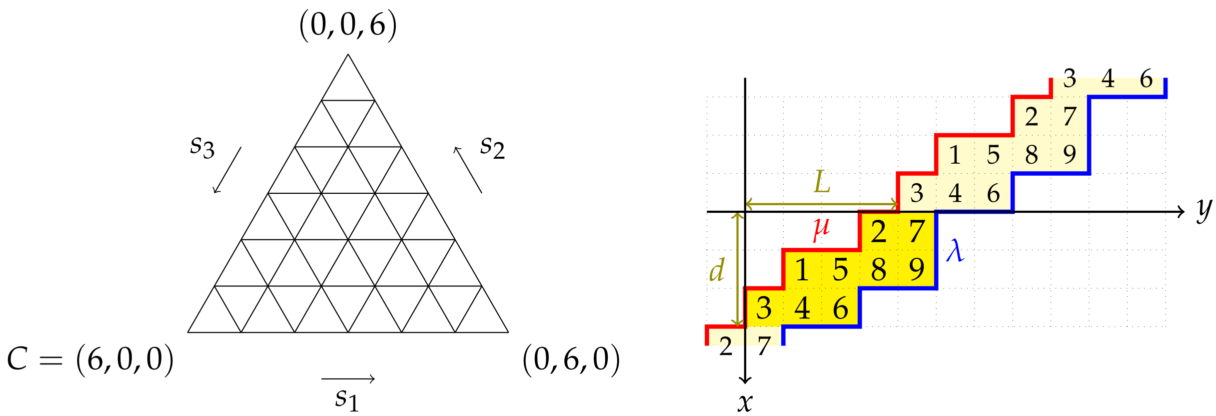

Figure 1: Left: The simplicial region $\Delta_{3,6}$. Right: An element of $\mathrm{SCT}_{3,4}(\lambda/\mu)$, where $\lambda = [5,5,3]$ and $\mu = [3,1,0]$ are shapes in $\Lambda_{3,4}$, and $|\lambda/\mu| = 9$.

The enumeration of n-step walks in $\mathcal{D}_{d,L}$ starting at a given $\mathbf{x} \in \Delta_{d,L}$ is relatively straightforward for $d = 2$ [7, Proposition 1, Corollary 2]. For $d = 3$, the problem was solved by Mortimer and Prellberg [7, Theorem 3]. In the special case of walks starting at C, they show that these walks are equinumerous with Motzkin paths of bounded height.

Recall that a Motzkin path of length n is a path in $\mathbb{Z}^2$ from $(0,0)$ to $(n,0)$, with steps $(1,1)$, $(1,0)$ and $(1,-1)$, not going below the x-axis. Let $M_{n,h}$ denote the number of Motzkin paths of length n and height at most h, that is, not going above the line $y = h$. Additionally, let $M'_{n,h}$ be the number of Motzkin paths of length n and height at most h that do not have any $(1,0)$ steps on the line $y = h$. For $n \geq 0$ and $L \geq 1$, let

$$a_{n,L} = \begin{cases} M_{n,h} & \text{if } L = 2h+1, \\ M'_{n,h} & \text{if } L = 2h. \end{cases} \tag{1.1}$$

Theorem 1.1 ([7]). *The number of n-step walks in $\mathcal{D}_{3,L}$ starting at C equals $a_{n,L}$.*

Mortimer and Prellberg's proof in [7] uses the kernel method to solve a functional equation. A complicated bijective proof of Theorem 1.1 has recently been given by Courtiel, Elvey Price and Marcovici [2], who also find an expression for the generating function for walks in $\mathcal{D}_{4,L}$ that start at a corner C. In the same paper, Courtiel *et al.* prove the following striking result.

Theorem 1.2 ([2]). *For any $\mathbf{x} \in \Delta_{d,L}$, there is a bijection between the set of n-step walks in $\mathcal{D}_{d,L}$ starting at $\mathbf{x}$ and the set of n-step walks in $\mathcal{D}_{d,L}$ ending at $\mathbf{x}$.*

The bijection in [2] is recursive, defined by repeatedly applying certain flips to adjacent steps. In Section 3, we will provide an arguably cleaner bijection by first interpreting walks as certain tableaux, and then translating a Robinson-Schensted algorithm for such tableaux into a bijection for walks in $\mathcal{D}_{d,L}$.

1.2 Standard cylindric tableaux

Cylindric partitions were introduced by Gessel and Krattenthaler in [4], as plane partitions satisfying certain constraints between the entries of the first and the last row. A particularly interesting special case of them, called $(0,1)$-cylindric partitions in [4], is equivalent to *semistandard cylindric tableaux*, as defined by Postnikov in [9]. These tableaux are related to the 3-point Gromov–Witten invariants, which are the structure constants of the quantum cohomology ring of the Grassmannian. Postnikov introduces a generalization of Schur functions, as generating functions for semistandard cylindric tableaux of a given shape, and he shows that, when these are expanded in terms of ordinary Schur functions, the Gromov–Witten invariants appear as coefficients in this expansion. These generalized Schur functions, under the name of *cylindric skew Schur functions*, have been further studied by McNamara [6] from the perspective of Schur-positivity.

Define the cylinder $\mathcal{C}_{d,L}$ to be the quotient $\mathbb{Z}^2/(-d,L)\mathbb{Z}^2$. Elements of $\mathcal{C}_{d,L}$ are equivalence classes $\langle i,j\rangle = (i,j) + (-d,L)\mathbb{Z}^2$, where $i,j \in \mathbb{Z}$, and they are called *cells*. We borrow this notation from [9, 8], although we use L instead of $d+L$ for the second index. As in [9, 8], we draw points $(i,j) \in \mathbb{Z}^2$ as unit squares on the plane with vertices $(i-1,j-1),(i-1,j),(i,j-1),(i,j)$, with the unusual convention that the positive x-axis points downward and the positive y-axis points to the right, to be consistent with the English notation for Young diagrams. With this 90°-rotation of the usual Cartesian coordinates, (i,j) represents the square in row i and column j, where row indices increase from top to bottom, and column indices increase from left to right.

A *cylindric shape*[2] *of period* (d,L) is a doubly infinite weakly decreasing sequence of integers, $\lambda = (\lambda_i)_{i\in\mathbb{Z}}$, such that $\lambda_i = \lambda_{i+d} + L$ for all $i \in \mathbb{Z}$. We often write it as $\lambda = [\lambda_1, \lambda_2, \ldots, \lambda_d]$, since these d integers uniquely determine a cylindric shape, provided that $\lambda_d + L \geq \lambda_1 \geq \lambda_2 \geq \cdots \geq \lambda_d$. For example, we write $\lambda = [5,5,3] = (\ldots,9,9,7,5,5,3,1,1,-1,\ldots) \in \Lambda_{3,4}$. Denote by $\Lambda_{d,L}$ the set of cylindric shapes of period (d,L). We will use the term *shape* to mean *cylindric shape* throughout the paper. For $\lambda \in \Lambda_{d,L}$, the region $\{(i,j) \in \mathbb{Z}^2 : j \leq \lambda_i\}$ is a union of equivalence classes. We denote it by $Y_\lambda = \{\langle i,j\rangle \in \mathcal{C}_{d,L} : j \leq \lambda_i\}$, and call it the *Young diagram* of λ.

For $\lambda, \mu \in \Lambda_{d,L}$, we write $\mu \subseteq \lambda$ if $Y_\mu \subseteq Y_\lambda$; equivalently, if $\mu_i \leq \lambda_i$ for all $i \in \mathbb{Z}$. For $\mu \subseteq \lambda$, we define the *cylindric Young diagram of shape* λ/μ to be the set

$$Y_{\lambda/\mu} = Y_\lambda \setminus Y_\mu = \{\langle i,j\rangle \in \mathcal{C}_{d,L} : \mu_i < j \leq \lambda_i\}.$$

Unlike Y_λ or Y_μ, the set $Y_{\lambda/\mu}$ is finite. We denote its cardinality by $|\lambda/\mu| = \sum_{i=1}^{d}(\lambda_i - \mu_i)$.

A *standard cylindric tableau* of shape λ/μ is a bijection $T\colon Y_{\lambda/\mu} \to \{1,2,\ldots,|\lambda/\mu|\}$ such that $T(\langle i,j\rangle) < T(\langle i+1,j\rangle)$ and $T(\langle i,j\rangle) < T(\langle i,j+1\rangle)$ for all i,j; equivalently, a

[2]Such an object is called a cylindric partition in [8], but we avoid this term because in [4] it is used to mean something different, namely the cylindric version of a plane partition

filling of the cells in $Y_{\lambda/\mu}$ so that entries are increasing along rows (from left to right) and along columns (from top to bottom). See the right of Figure 1 for an example. Denote by $\mathrm{SCT}_{d,L}(\lambda/\mu)$ the set of standard cylindric tableaux of shape λ/μ, where $\lambda, \mu \in \Lambda_{d,L}$. If $T \in \mathrm{SCT}_{d,L}(\lambda/\mu)$, we call λ and μ the *outer shape* and the *inner shape* of T, respectively. Denote by $\mathrm{SCT}^n_{d,L}(\cdot/\mu)$ (respectively $\mathrm{SCT}^n_{d,L}(\lambda/\cdot)$) the set of standard cylindric tableaux with n cells and inner shape μ (respectively outer shape λ).

We construct an infinite directed graph $\mathcal{P}_{d,L}$ whose vertex set $\Lambda_{d,L}$ as follows. For $\mu, \lambda \in \Lambda_{d,L}$, there is an edge from μ to λ if Y_λ can be obtained from Y_μ by adding a cell; equivalently, if $\lambda_i = \mu_i + 1$ for some i and $\lambda_j = \mu_j$ for all $j \neq i$, where $1 \leq i, j \leq d$. Note that it is possible to add a cell to row i of Y_μ if and only if $\mu_{i-1} > \mu_i$.

1.3 Exclusion processes

In the *totally asymmetric simple exclusion process* (TASEP) on the cycle $\mathbb{Z}_N$, each of the sites $j \in \mathbb{Z}_N$ can either contain a particle or be empty. We denote a state of the system by $u = u_1 u_2 \cdots u_N$, where $u_j = 1$ if site j contains a particle, and $u_j = 0$ otherwise. The indices of u are always interpreted modulo N. We draw such a state by placing N beads around a circle representing the sites in clockwise order, starting and ending at the bottom of the circle, and filling in the beads corresponding to particles. At each time step, a particle can jump to the next site in counterclockwise direction if this site is empty. The number of particles remains fixed through the process, let d denote this number, and assume that $d \geq 1$.

Typically, one associates transition probabilities to these particle jumps to define a Markov chain [3]. Here, however, we are interested in the underlying directed graph $\mathcal{E}_{d,N-d}$ whose vertices are the $\binom{N}{d}$ states $u = u_1 u_2 \cdots u_N$ containing d particles, and whose edges correspond to valid jumps of a particle. Specifically, $\mathcal{E}_{d,N-d}$ has an edge from state u to state v if and only if there exists $j \in [N]$ such that $u_{j-1}u_j = 01$, $v_{j-1}v_j = 10$, and $u_k = v_k$ for all $k \in \mathbb{Z}_N \setminus \{j-1, j\}$, with indices taken modulo N. Note that $\mathcal{E}_{d,N-d}$ does not contain loops, unlike the Markov chain for the TASEP, where each of the N sites is equally likely to *attempt* a jump, but it succeeds only if that site contains a particle and the next site counterclockwise is empty, and it stays in the same state otherwise. Thus, in the TASEP Markov chain, each of the edges in $\mathcal{E}_{d,N-d}$ gets assigned probability $1/N$, while the loop from a state to itself has positive probability.

Let us now construct a directed multigraph $\mathcal{N}_{d,N-d}$, which is a quotient of $\mathcal{E}_{d,N-d}$ under the equivalence relation given by cyclic rotations. Specifically, define a *necklace* to be an equivalence class of vertices of $\mathcal{E}_{d,N-d}$, where $u \sim v$ if there exists k such that $u_j = v_{j+k}$ for all j, again with indices taken modulo N. The vertices of $\mathcal{N}_{d,N-d}$ are necklaces, for which we use the notation $[u]$. The number of edges from necklace $[u]$ to necklace $[v]$ is the number of states $\widehat{v} \in [v]$ for which $\mathcal{E}_{d,N-d}$ has an edge from u to $\widehat{v}$. Note that, by cyclic symmetry, this number does not depend on the chosen representative from $[u]$. In other words, $[u]$ has an outgoing edge for each cyclic occurrence of the consecutive substring 01 in the necklace, and the edge points to the necklace obtained from $[u]$ by replacing this occurrence with 10.

The graph $\mathcal{E}_{3,3}$ and the multigraph $\mathcal{N}_{3,3}$ appear in Figure 2(c)(d).

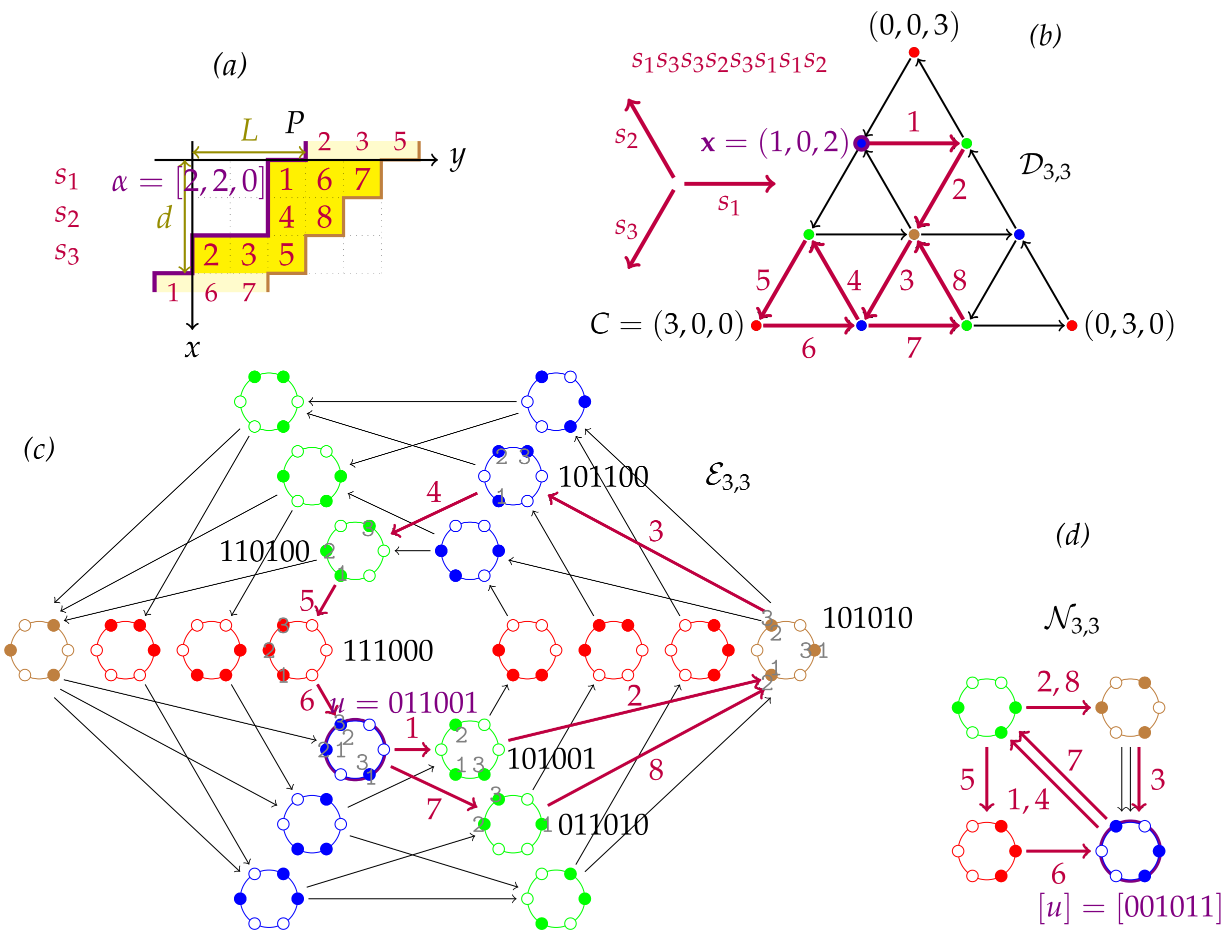

Figure 2: A standard cylindric tableau P with inner shape $\alpha = [2,2,0] \in \Lambda_{3,3}$ *(a)*, the corresponding walk in $\mathcal{D}_{3,3}$ starting at $\mathbf{x} = (1,0,2)$ *(b)*, the one in $\mathcal{E}_{3,3}$ starting at $u = 011001$ *(c)*, and the one in the multigraph $\mathcal{N}_{3,3}$ starting at $[u] = [001011]$ *(d)*.

2 Connecting all three

In this section we provide bijections that relate walks in simplices, standard cylindric tableaux, and exclusion processes. The idea behind the bijections is that inserting a cell in row i of a shape in $\Lambda_{d,L}$ translates to moving along a step s_i in $\mathcal{D}_{d,L}$, and to the ith particle (with the appropriate indexing) of a state in $\mathcal{E}_{d,L}$ or $\mathcal{N}_{d,L}$ jumping to the next site in counterclockwise direction. Next we make this precise.

Unlike in previous appearances of tableaux in connection to the TASEP in the literature [1, 5], where certain tableaux are used to encode states, our standard cylindric tableaux encode sequences of states (*i.e.*, walks in the Markov chain) instead.

The bijections are based on the construction of *covering maps*, that is, surjective maps from the set of vertices of a directed multigraph to the set of vertices of another, that induce bijections between the outgoing edges of each vertex and those of its image.

Lemma 2.1. *The following are covering maps:*

(i) The map $f\colon \mathcal{P}_{d,L} \to \mathcal{D}_{d,L}$ defined on the vertices $\alpha = [\alpha_1, \alpha_2, \ldots, \alpha_d] \in \Lambda_{d,L}$ by

$$f(\alpha) = (\alpha_0 - \alpha_1, \alpha_1 - \alpha_2, \ldots, \alpha_{d-1} - \alpha_d).$$

(ii) The map $g\colon \mathcal{D}_{d,L} \to \mathcal{N}_{d,L}$ defined on the vertices $\mathbf{x} = (x_1, x_2, \ldots, x_d) \in \Delta_{d,L}$ by

$$g(\mathbf{x}) = [0^{x_1}10^{x_2}1 \cdots 0^{x_d}1].$$

(iii) The quotient map $q\colon \mathcal{E}_{d,L} \to \mathcal{N}_{d,L}$ obtained by taking equivalence classes of states $u = u_1u_2\cdots u_{d+L}$ under cyclic rotation, as described in Section 1.3.

In Figure 2, the covering maps $g\colon \mathcal{D}_{d,L} \to \mathcal{N}_{d,L}$ and $q\colon \mathcal{E}_{d,L} \to \mathcal{N}_{d,L}$ are illustrated by the colors of the vertices: each vertex of $\mathcal{N}_{d,L}$ has the same color as each of its preimages.

Lemma 2.2. *Let $f\colon G \to H$ be a covering map between directed multigraphs. Then, for any vertex u of V and any $n \geq 0$, f induces a bijection $\widetilde{f}$ between n-step walks in G starting at u and n-step walks in H starting at $f(u)$.*

Theorem 2.3. *Fix $d, L \geq 1$. Let $\alpha \in \Lambda_{d,L}$, let $\mathbf{x} = (x_1, x_2, \ldots, x_d) \in \Delta_{d,L}$ where $x_i = \alpha_{i-1} - \alpha_i$ for $1 \leq i \leq d$, and let $u = 0^{x_1}10^{x_2}1 \cdots 0^{x_d}1$. There are natural bijections between the following:*

(a) The set $\mathrm{SCT}^n_{d,L}(\cdot/\alpha)$.

(b) The set of n-step walks in $\mathcal{D}_{d,L}$ starting at vertex $\mathbf{x}$.

(c) The set of n-step walks in $\mathcal{E}_{d,L}$ starting at state u.

(d) The set of n-step walks in $\mathcal{N}_{d,L}$ starting at state $[u]$.

Proof. To describe a bijection between the sets *(a)* and *(b)*, we use the covering map $f\colon \mathcal{P}_{d,L} \to \mathcal{D}_{d,L}$ from Lemma 2.1(i), which satisfies $f(\alpha) = \mathbf{x}$. Indeed, a tableau $T \in \mathrm{SCT}^n_{d,L}(\cdot/\alpha)$ can be interpreted as a walk in $\mathcal{P}_{d,L}$ starting at α, given by the sequence of shapes $\alpha = \lambda^{(0)} \subset \lambda^{(1)} \subset \cdots \subset \lambda^{(n)}$, where each $\lambda^{(r)}$ is the outer shape of the standard cylindric tableau consisting of the cells of T with entries at most r. The bijection $\widetilde{f}$ from *(a)* to *(b)* that results from this covering map by applying Lemma 2.2 can be described directly as follows. Given $T \in \mathrm{SCT}^n_{d,L}(\cdot/\alpha)$, let i_r be the row that contains entry r, for each $1 \le r \le n$. Then $\widetilde{f}(T)$ is the n-step walk in $\Delta_{d,L}$ that starts at $\mathbf{x}$ and has steps $s_{i_1} s_{i_2} \cdots s_{i_n}$. See Figure 2 for an example. The condition that T has increasing rows and columns guarantees that the walk stays inside the region $\Delta_{d,L}$.

A bijection $\widetilde{g}$ between the sets *(b)* and *(d)* arises from the covering map $g \colon \mathcal{D}_{d,L} \to \mathcal{N}_{d,L}$ from Lemma 2.1(ii), which satisfies $g(\mathbf{x}) = [u]$, using again Lemma 2.2. A bijection $\widetilde{q}$ between *(c)* and *(d)* is immediate from the quotient map q in Lemma 2.1(i).

It is also not hard to describe direct bijections between *(a)* and *(c)* and between *(b)* and *(c)*. For example, indexing the particles in state u so that particle i occupies the site corresponding to the ith 1 from the left, the walk in $\mathcal{E}_{d,L}$ starting at u that corresponds to the above $T \in \mathrm{SCT}^n_{d,L}(\cdot/\alpha)$ consists of successive jumps of the particles $i_1, i_2, \ldots, i_n$ in counterclockwise direction. □

Conjugation of standard cylindric tableaux is the involution obtained by reflecting along the diagonal $y = x$. For $\alpha \in \Lambda_{d,L}$, define its conjugate to be the shape $\alpha' \in \Lambda_{L,d}$, where $\alpha'_j = \max\{i : \alpha_i \ge j\}$ for all j. If T is a standard cylindric tableau of shape λ/μ, define its conjugate to be the standard cylindric tableau T' of shape λ'/μ' where $T'(\langle j,i \rangle) = T(\langle i,j \rangle)$ for all $\langle i,j \rangle$. For a state $u = u_1 u_2 \cdots u_N$ of the TASEP on $\mathbb{Z}_N$, its reverse-complement u^{rc} is the state where $u^{rc}_i = 1 - u_{N+1-i}$ for all i, obtained from u by applying particle-hole symmetry, *i.e.*, switching occupied sites with empty sites and reversing the orientation. The following result follows easily from the bijections in Theorem 2.3 by conjugation at the level of tableaux. See Figure 3 for an example.

Theorem 2.4. *With the notation from Theorem 2.3, let $\alpha' \in \Lambda_{L,d}$ be the conjugate of α, let $\mathbf{y} = (y_1, y_2, \ldots, y_L) \in \Delta_{L,d}$ where $y_j = \alpha'_{j-1} - \alpha'_j$ for $1 \le j \le L$, and let u^{rc} be the reverse-complement of u. There are natural bijections between the sets in Theorem 2.3 and the following:*

(a′) The set $\mathrm{SCT}^n_{L,d}(\cdot/\alpha')$.

(b′) The set of n-step walks in $\mathcal{D}_{L,d}$ starting at vertex $\mathbf{y}$.

(c′) The set of n-step walks in $\mathcal{E}_{L,d}$ starting at state u^{rc}.

(d′) The set of n-step walks in $\mathcal{N}_{L,d}$ starting at state $[u^{rc}]$.

While the bijections between the sets *(a)* and *(a′)*, and between *(d)* and *(d′)*, are relatively straightforward, the bijection between *(b)* and *(b′)* that results from Theorem 2.4 has no simple description directly in terms of walks in simplices.

As a consequence of these bijections and Theorem 1.1, we see that the number $a_{n,L}$ of Motzkin paths of bounded height, as given by Equation (1.1), also counts standard cylindric tableaux of period $(3, L)$ with n cells and rectangular inner shape $[0,0,0]$, n-step walks in $\mathcal{D}_{3,L}$ starting at a corner C, n-step walks in $\mathcal{D}_{L,3}$ starting at a corner C, n-step walks in $\mathcal{E}_{3,L}$ starting at $1^3 0^L$, and n-step walks in $\mathcal{N}_{3,L}$ starting at $[1^3 0^L]$.

Similarly, we deduce that the coefficients of the generating function given in [2, Corollary 39] enumerate each of the sets in Theorems 2.3 and 2.4 where $d = 4$, $\alpha = [0,0,0,0]$, $\mathbf{x}$ and $\mathbf{y}$ are corners of the corresponding simplices, and $u = 1^4 0^L$.

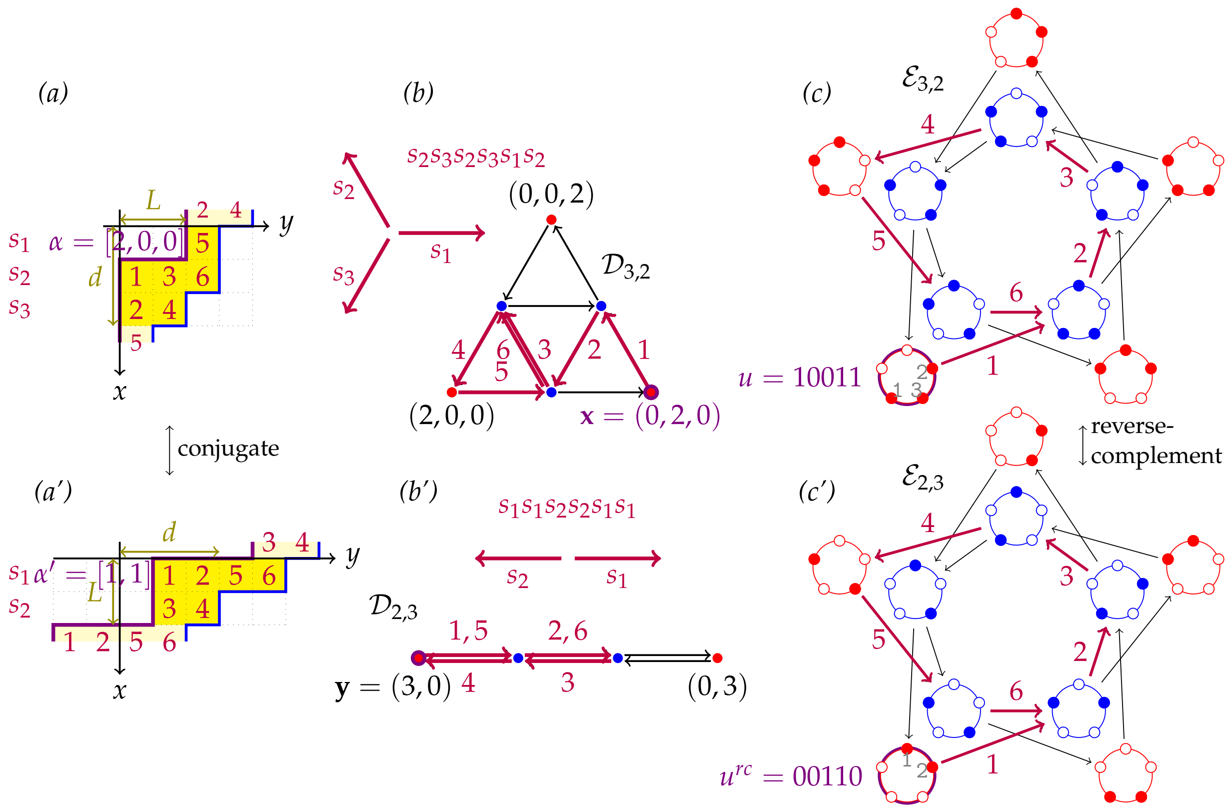

Figure 3: A standard cylindric tableau with inner shape $\alpha = [2,0,0] \in \Lambda_{3,2}$ *(a)*, and its conjugate with inner shape $\alpha' = [1,1] \in \Lambda_{2,3}$ *(a′)*; the corresponding walks in $\mathcal{D}_{3,2}$ starting at $\mathbf{x} = (0,2,0)$ *(b)*, and in $\mathcal{D}_{2,3}$ starting at $\mathbf{y} = (3,0)$ *(b′)*; and the corresponding walks in $\mathcal{E}_{3,2}$ starting at $u = 10011$ *(c)*, and in $\mathcal{E}_{2,3}$ starting at $u^{rc} = 00110$ *(c′)*.

3 Schensted insertion, and a bijection between forward and backward walks

Sagan and Stanley [10] introduced analogues of the Robinson–Schensted algorithm for skew tableaux. They defined two row insertion operations, later extended by Neyman [8] to cylindric tableaux. In a nutshell, *internal row insertion* removes an inner corner (namely, a cell $\langle i, \mu_i + 1\rangle$ such that $\mu_{i-1} > \mu_i$, where μ is the inner shape), and successively inserts the removed entry into the next row, possibly bumping another entry to the following row, until the inserted entry is placed at the end of a row. See Figure 4 for an example.

The algorithms work in the semistandard case, where the entries of the tableaux can be any multiset of positive integers as long as rows are weakly increasing and columns are strictly increasing. Next we state the main correspondence in the special case of standard cylindric tableaux, since they correspond naturally to walks in simplices.

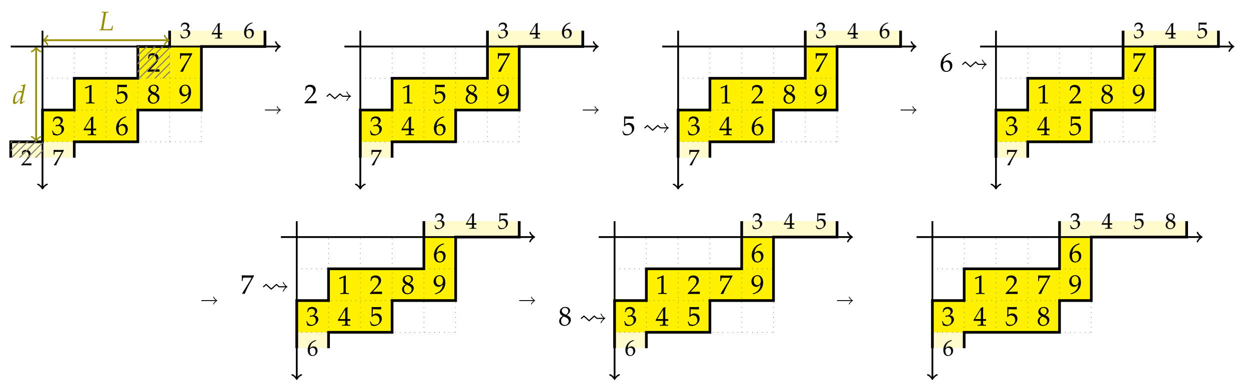

Figure 4: Internal insertion at row 1 in the standard cylindric tableau from Figure 1.

Theorem 3.1 ([8], extending [10])**.** *Fix $\alpha, \beta \in \Lambda_{d,L}$ and $n, m \geq 0$. There is a bijection, denoted by* CRSK*:*

$$\bigsqcup_{\substack{\mu \subseteq \alpha,\beta \\ |\alpha/\mu|=n, \\ |\beta/\mu|=m}} \mathrm{SCT}_{d,L}(\alpha/\mu) \times \mathrm{SCT}_{d,L}(\beta/\mu) \to \bigsqcup_{\substack{\lambda \supseteq \alpha,\beta \\ |\lambda/\beta|=n, \\ |\lambda/\alpha|=m}} \mathrm{SCT}_{d,L}(\lambda/\beta) \times \mathrm{SCT}_{d,L}(\lambda/\alpha).$$

Proof sketch. Suppose that $|\alpha| + m = |\beta| + n$, since otherwise both unions are empty. Fix $\mu \subseteq \alpha, \beta$ with $|\alpha/\mu| = n$ and $|\beta/\mu| = m$, and let $(T, U) \in \mathrm{SCT}_{d,L}(\alpha/\mu) \times \mathrm{SCT}_{d,L}(\beta/\mu)$. We construct a sequence of pairs (P_k, Q_k) for $0 \leq k \leq m$. For $k = 0$, let $P_0 = T$, and let Q_0 be the empty tableau of shape α/α. For k from 1 to m, construct (P_k, Q_k) iteratively as follows. Let $\langle i, j \rangle$ be the cell in U containing k, which must be an inner corner of P_{k-1}. Let P_k be obtained from P_{k-1} by internal row insertion in $\langle i, j \rangle$, and let Q_k be obtained from Q_{k-1} by placing k in the cell where this insertion procedure terminates (*i.e.*, the cell that is added to the outer shape of P_{k-1} to obtain P_k). Finally, let $\mathrm{CRSK}(T, U) = (P_m, Q_m)$. □

Note that cylindric tableaux of period $(d, L) = (\infty, \infty)$ are equivalent to (non-cylindric) skew tableaux, so Theorem 3.1 reduces to [10, Theorem 5.1] in the special case that $\pi = \emptyset$. It is shown in [8, Theorem 5.18], generalizing [10, Theorem 3.3], that if $\mathrm{CRSK}(T, U) = (P, Q)$, then $\mathrm{CRSK}(U, T) = (Q, P)$. In particular, in the case $\alpha = \beta$, taking $T \in \mathrm{SCT}_{d,L}(\alpha/\mu)$ where $|\alpha/\mu| = n$, we have $\mathrm{CRSK}(T, T) = (P, P)$, for some $P \in \mathrm{SCT}_{d,L}(\lambda/\alpha)$ where $|\lambda/\alpha| = n$. We denote by ϕ the map such that $\phi(T) = P$ in this case. For any fixed $\alpha \in \Lambda_{d,L}$, this map is a bijection

$$\phi \colon \mathrm{SCT}^n_{d,L}(\alpha/\cdot) \to \mathrm{SCT}^n_{d,L}(\cdot/\alpha). \tag{3.1}$$

See Figure 5 for an example.

Aside from conjugation, another natural involution on the set $\Lambda_{d,L}$ is given by 180° rotation. For $\lambda = [\lambda_1, \lambda_2, \ldots, \lambda_d] \in \Lambda_{d,L}$, define its *complement* to be $\overline{\lambda} = [L - \lambda_d, L -$

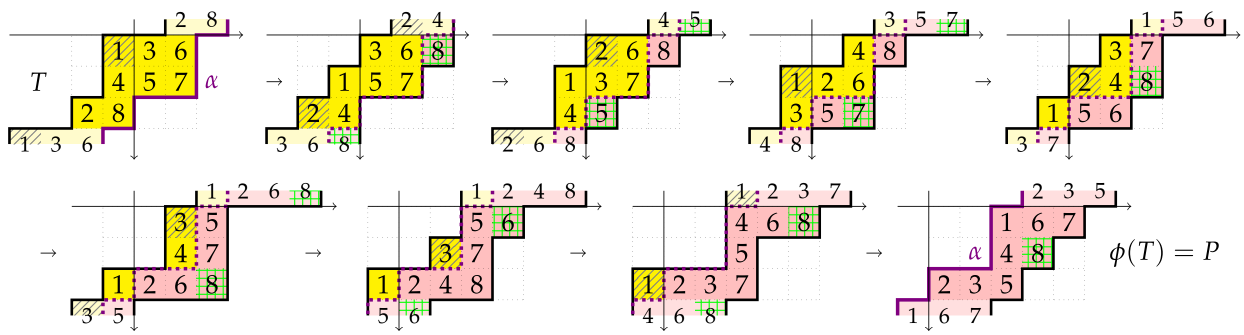

Figure 5: An example of the bijection $\phi\colon \mathrm{SCT}_n(\alpha/\cdot) \to \mathrm{SCT}_n(\cdot/\alpha)$, with $d = 3$, $L = 3$, $n = 8$, $\alpha = [2,2,0]$. The inner corners where internal insertion is about to occur are shaded with gray diagonal lines, and the newly added cells where the previous insertion terminated are highlighted with a green grid pattern.

$\lambda_{d-1}, \ldots, L - \lambda_1] \in \Lambda_{d,L}$. For $\langle i,j\rangle \in \mathcal{C}_{d,L}$, define $\overline{\langle i,j\rangle} = \langle d+1-i, L+1-j\rangle$. Then, for $\lambda, \mu \in \Lambda_{d,L}$, we have $\mu \subseteq \lambda$ if and only if $\overline{\lambda} \subseteq \overline{\mu}$, and $\langle i,j\rangle \in Y_{\lambda/\mu}$ if and only if $\overline{\langle i,j\rangle} \in Y_{\overline{\mu}/\overline{\lambda}}$. For $T \in \mathrm{SCT}(\lambda/\mu)$ with $|\lambda/\mu| = n$, define its *complement* tableau $\overline{T} \in \mathrm{SCT}(\overline{\mu}/\overline{\lambda})$ to be the one with entries $\overline{T}(\overline{\langle i,j\rangle}) = n + 1 - T(\langle i,j\rangle)$ for all $\langle i,j\rangle \in Y_{\lambda/\mu}$. Viewing tableaux as fillings of the cells in the cylindric Young diagram, $\overline{T}$ is obtained from T by performing a 180° rotation and replacing each entry k with $n+1-k$.

The following property of ϕ, illustrated in Figure 6, follows from [8, Corollary 4.19].

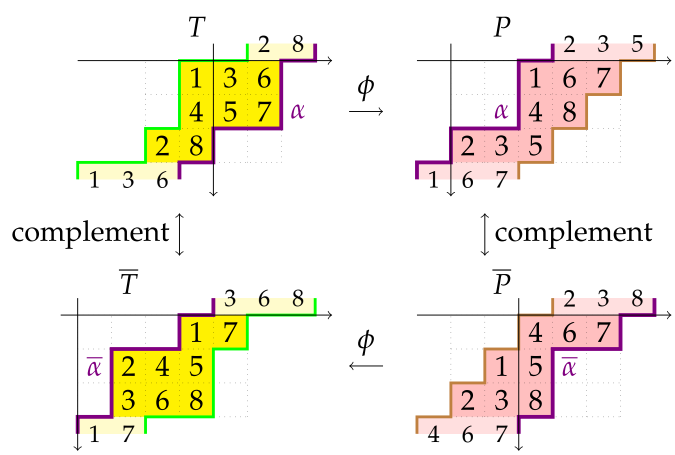

Figure 6: The above diagram commutes by Proposition 3.2.

Proposition 3.2 ([8]). *For any standard cylindric tableau P, we have $\phi^{-1}(P) = \overline{\phi(\overline{P})}$.*

The reason for this symmetry is that each internal insertion in the computation of ϕ can be undone by performing internal insertion in the complement tableau at the newly created cell. Thus, all the steps in the description of ϕ are reversed when applying ϕ to the complement tableau.

In [2], Courtiel *et al.* give a recursive bijection to prove Theorem 1.2, by repeatedly applying certain flips to adjacent steps and to the last step of the walk, until all the forward steps have been switched into backward steps. An alternative description of this bijection is also given in [2, Sec. 2.3], as a tiling of an $n \times n$ square with labeled tiles that must follow certain rules that emulate the allowed flips in the walks.

Our setting provides a canonical, non-recursive bijective proof of Theorem 1.2. Indeed, our Schensted-insertion-based map ϕ, when translated in terms of walks in $\mathcal{D}_{d,L}$ via the correspondence in Theorem 2.3, provides the desired bijection. Additionally, by Proposition 3.2, the map $P \mapsto \phi(\overline{P})$ is an involution. It would be interesting to determine how our map ϕ compares to the recursive construction from [2], as it is conceivable that they are different descriptions of the same bijection.

The following theorem translates the resulting equivalence to the various settings. Figure 7 shows an example of these bijections.

Theorem 3.3. *With the notation from Theorem 2.3, there are bijections between the sets (a)–(d) and the following:*

(a″) The set $\mathrm{SCT}^n_{d,L}(\alpha/\cdot)$.

(b″) The set of n-step walks in $\mathcal{D}_{d,L}$ *ending at vertex* $\mathbf{x}$.

(c″) The set of n-step walks in $\mathcal{E}_{d,L}$ *ending at state* u.

(d″) The set of n-step walks in $\mathcal{N}_{d,L}$ *ending at state* $[u]$.

References

[1] S. Corteel, O. Mandelshtam, and L. Williams. "From multiline queues to Macdonald polynomials via the exclusion process". *Sém. Lothar. Combin.* **82B** (2020), Art. 97, 12.

[2] J. Courtiel, A. Elvey Price, and I. Marcovici. "Bijections between walks inside a triangular domain and Motzkin paths of bounded amplitude". *Electron. J. Combin.* **28**.2 (2021), Paper No. 2.6, 44. DOI.

[3] P. A. Ferrari and J. B. Martin. "Stationary distributions of multi-type totally asymmetric exclusion processes". *Ann. Probab.* **35**.3 (2007), pp. 807–832. DOI.

[4] I. M. Gessel and C. Krattenthaler. "Cylindric partitions". *Trans. Amer. Math. Soc.* **349**.2 (1997), pp. 429–479. DOI.

[5] O. Mandelshtam. "Toric tableaux and the inhomogeneous two-species TASEP on a ring". *Adv. in Appl. Math.* **113** (2020), pp. 101958, 50. DOI.

[6] P. McNamara. "Cylindric skew Schur functions". *Adv. Math.* **205**.1 (2006), pp. 275–312. DOI.

[7] P. R. G. Mortimer and T. Prellberg. "On the number of walks in a triangular domain". *Electron. J. Combin.* **22**.1 (2015), Paper 1.64, 15.

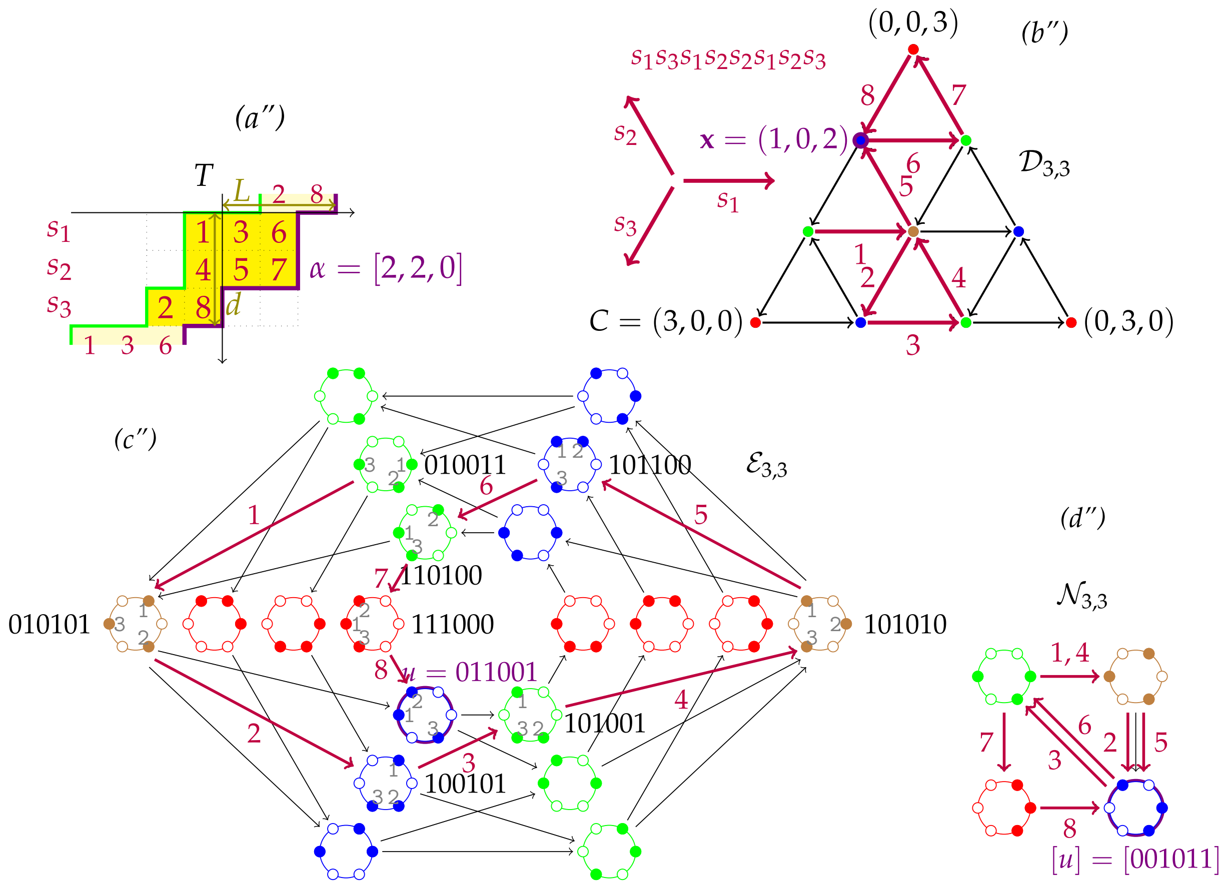

Figure 7: When the bijections from Theorem 3.3 are applied to the objects in Figure 2, we obtain a standard cylindric tableau $T = \phi^{-1}(P)$ with outer shape $\alpha = [2,2,0] \in \Lambda_{3,3}$ *(a″)*, a walk in $\mathcal{D}_{3,3}$ ending at $\mathbf{x} = (1,0,2)$ *(b″)*, a walk in $\mathcal{E}_{3,3}$ ending at $u = 011001$ *(c″)*, and a walk in $\mathcal{N}_{3,3}$ ending at $[u] = [001011]$ *(d″)*.

[8] E. Neyman. "Cylindric Young Tableaux and their Properties". 2015. arXiv:1410.5039.

[9] A. Postnikov. "Affine approach to quantum Schubert calculus". *Duke Math. J.* **128**.3 (2005), pp. 473–509. DOI.

[10] B. E. Sagan and R. P. Stanley. "Robinson-Schensted algorithms for skew tableaux". *J. Combin. Theory Ser. A* **55**.2 (1990), pp. 161–193. DOI.